STATIONARY FRAME ACTIVE POWER FILTER CONTROL BASED ON MULTIRESOLUTION ANALYSIS

Mihai Culea, Teodor Dumitriu, Mihai Nichita, Traian Munteanu

"Dunărea de Jos" University of Galati, Romania
Advanced Control Systems Research Center
111, Domnească, 800201-Galați, Romania; email:teodor.dumitriu@ugal.ro

Abstract: The paper presents an active power filter control method. The reference signal is generated in the stationary reference frame α-β using multiresolution analysis and the controllers used are P-resonant controllers, suitable for this particular application due to the fact that the steady-state error is zero for sinusoidal references with the frequency corresponding to the resonant frequency of the controller.

Keywords: active power filter, multiresolution analysis, resonant controller.

1. INTRODUCTION

With the proliferation of nonlinear loads such as power electronic equipments or arc furnaces, the amount of current harmonics has increased (Dugan *et al.*, 1996). This causes the alteration of the power quality beyond acceptable level in many situations. Therefore the active power filter (APF) as an efficient solution to improve the power quality has been brought as an increasing concern (Akagi, 1995), (Rastogi *et al.*, 1994). Compared with passive power filters, active power filters can dynamically compensate harmonics, reactive power and unbalance produced by varying loads (Fujita *et al.*, 1991). In addition, resonance phenomena and several other serious problems caused by passive filters can also be avoided (Rastogi *et al.*, 1994).
The principle of the APF (figure 1) is that it behaves as a controlled current source, and is used to directly cancel harmonic currents arising from a non-linear load. However, this presents two immediate problems, namely:
1) the precise control of the active filter current to match the reference value
2) the derivation of the reference value for the ASF
Several methods exist to derive the harmonic references, including the use of PQ theory, measured voltage and known impedance at the point of common connection (PCC) (Sato *et al.*, 1999), and the more simple direct measurement and filtering of the load current (Buso *et al.*, 1998).

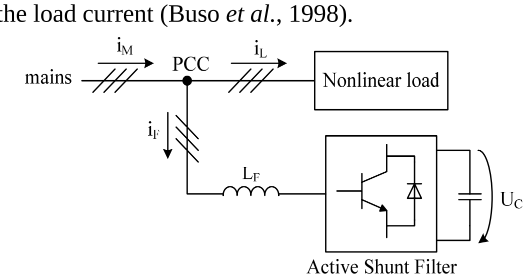

Fig.1. Active shunt structure

In order to increase the precision of the ASF a method of control is proposed based on the stationary frame control. The reference is generated using multiresolution analysis and, since the reference is sinusoidal, the controllers used are resonant controllers which have a zero steady state error for sinusoidal references (Zmood *et al.*, 2003).

2. CONTROL SCHEME DESCRIPTION

The issue of precise current control has been looked upon in many papers and the methods employed range from hysteresis control (Malesani *et al.*, 1997)

to predictive control (Lu et al., 1998).
The use of rotating reference frame, either simple or multiple, is a widely used control method, mainly because by shifting the references in the d-q plane a sinusoidal reference is transformed into a continuous one, thus allowing the use of PI controllers (Butt *et al.*, 1999). The control block is presented in figure 2. the phase locked loop (PLL) is needed to determine the electric angle.

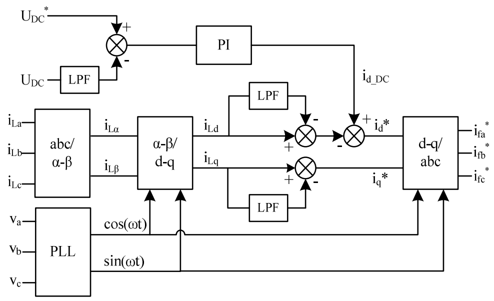

Fig.2. Control block for the synchronous rotating frame

If the low pass filter (LPF) is omitted for the iq current then the ASF can compensate the reactive power as well.
There are however several drawbacks given by the fact that the exact electrical angle is needed and the reference signal is not just continuous but it also has *6k* harmonic components. For these components the PI controllers determine an important phase shift. Moreover, there is a cross-coupling term linking the id and iq channels.
An alternative method for controlling the ASF is the use of fixed reference frame. By using only the Clarke transform, presented in equation 1, a three phase system is transformed into a two-phase system in the α-β stationary frame

$$(1)\quad \begin{bmatrix} x_\alpha \\ x_\beta \end{bmatrix} = \sqrt{\frac{2}{3}} \begin{bmatrix} 1 & -\frac{1}{2} & -\frac{1}{2} \\ 0 & \frac{\sqrt{3}}{2} & -\frac{\sqrt{3}}{2} \end{bmatrix} \begin{bmatrix} x_{an} \\ x_{bn} \\ x_{cn} \end{bmatrix}$$

For the stationary frame control there is no need to use a PLL and there isn't a cross-coupling term, which simplifies the control (figure 3).

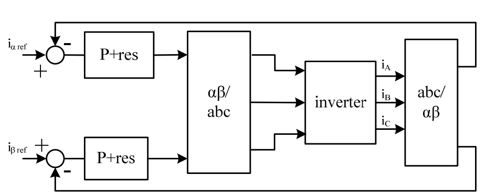

Fig.3. Control block for stationary reference frame

The main drawback of this structure is due to the fact that the reference signal is sinusoidal. PI controllers introduce a stationary error when used for sinusoidal reference.

To overcome this, a resonant controller is used. The PI controller has an infinite gain for a DC component, therefore, in order to obtain a zero steady-state error at a given frequency the system's gain has to be very large at that specific instant (Zmood *et al.*, 2003).

A P-resonant controller has this particular propriety. Its transfer function is:

$$(2)\quad H_{AC}(s) = K_p + \frac{2K_i s}{s^2 + \omega_0^2}$$

where ω_0 is the resonant frequency of the controller. A modified P-resonant controller was proposed by Fukuoka and it has the transfer function:

$$(3)\quad H_{AC}(s) = K_p + \frac{K_i \omega_0}{s^2 + \omega_0^2}$$

The Bode diagrams of the resonant controllers are presented in figure 4 and show a resonance around ω_0 frequency.

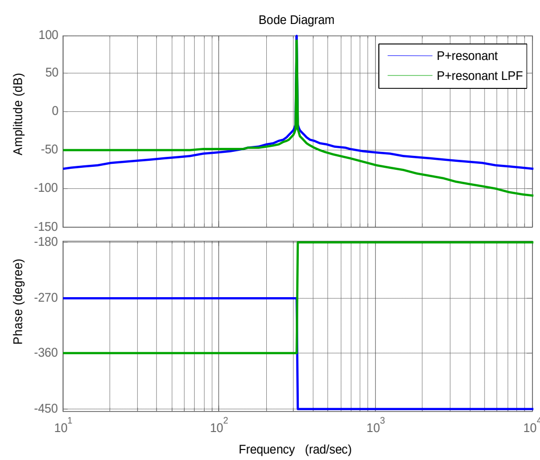

Fig.4. Bode diagram of the P-resonant controllers

Therefore the P-resonant controller has a zero steady-state error for the resonant frequency and it can be used for sinusoidal references.

3. APF REFERENCE GENERATION

Determining the reference is an important issue in APF control.
In the stationary reference frame the harmonic components and the fundamental are sinusoidal quantities so the Fourier analysis can be used to separate them. However, this can lead to unsatisfactory results for systems where the

frequency is varying, such as insular systems or weak networks. For such systems, a time-frequency signal analysis method can be used.

3.1. Multiresolution analysis

The wavelet is a continuous time signal that satisfies the following properties (Burrus, *et al*, 1997):

$$(4)\ \int_{-\infty}^{\infty} \psi(t)\mathrm{d}t = 0$$

$$(5)\ \int_{-\infty}^{\infty} \left|\psi(t)\right|^2 \mathrm{d}t < \infty$$

where $\psi(t)$ is defined as the mother wavelet. The continuous wavelet transform (CWT) associated with this wavelet is defined as:

$$(6)\ W(a,b) = \int_{-\infty}^{\infty} y(t)\psi_{a,b}^{*}(t)\mathrm{d}t$$

where $y(t)$ is any square integrable function, a is the scaling parameter, b is the translation parameter and $\psi_{a,b}(t)$ is the dilation and translation of the mother wavelet defined as:

$$(7)\ \psi_{a,b}(t) = \frac{1}{\sqrt{|a|}}\psi\left(\frac{t-b}{a}\right)$$

The signal $y(t)$ can be reconstructed from the CWT provided the mother wavelet satisfies the admissibility condition

$$(8)\ C = \int_{-\infty}^{\infty} \frac{\left|\Psi(\omega)\right|^2}{|\omega|}\mathrm{d}\omega < \infty$$

where $\Psi(\omega)$ is the Fourier Transform of $\psi(t)$. The reconstructed signal $y(t)$ is then:

$$(9)\ y(t) = \frac{1}{C}\int_{-\infty}^{\infty}\int_{-\infty}^{\infty} \frac{1}{|a|^2} W(a,b)\psi_{a,b}(t)\mathrm{d}a\mathrm{d}b$$

The CWT provides a redundant representation of the signal because the entire support of $W(a,b)$ is used in recovering $y(t)$, but this it isn't always necessary.

By evaluating the CWT at dyadic intervals the signal can be represented compactly as

$$(10)\ y(t) = \sum_{k=-\infty}^{\infty}\sum_{j=-\infty}^{\infty} d_j(k) 2^{\frac{j}{2}}\psi\left(2^j t - k\right)$$

where $d_j(k)$ are called the discrete wavelet transform (DWT) coefficients of $y(t)$.

Associated with the wavelet is a scaling function $\varphi(t)$ which, along with the wavelet, creates a multiresolution analysis (MRA) of the signal. An MRA consists of the nested linear vector space $\ldots \subset V_{-1} \subset V_0 \subset V_1 \subset \ldots$ such that:

1. $\bigcup_{j=-\infty}^{\infty} V_j$ is dense in the space of square integrable functions, $L^2(\mathbb{R})$;

2. $\bigcap_{j=-\infty}^{\infty} V_j = \{0\}$

3. If $y(t) \in V_j$ then $y(2t) \in V_{j+1}$ and vice-versa

4. There is a function $\varphi(t)$ such that its integer translates are a basis for V_0 that spans V_0.

The subspace span generated by the wavelet $\psi(t)$ is the orthogonal complement of V_0 and is defined as:

$$(11)\ V_1 = V_0 \oplus W_0$$

The scaling function of one level can be represented as a sum of the scaling functions of the next finer level:

$$(12)\ \varphi(t) = \sum_{n=-\infty}^{\infty} h(n)\sqrt{2}\varphi(2t-n)$$

The wavelet is also related to the scaling function by:

$$(13)\ \psi(t) = \sum_{n=-\infty}^{\infty} g(n)\sqrt{2}\varphi(2t-n)$$

where $h(n)$ and $g(n)$ are the coefficients of a low pass filter and a high pass filter respectively.

The scaling and the wavelet coefficients of a signal $y(t)$ can be evaluated using a filter bank of quadrature mirror filters (QMF) (Burrus *et al.*,1998):

$$(14)\ c_j(k) = \sum_{m=-\infty}^{\infty} c_{j+1}(m)h(m-2k)$$

$$(15)\ d_j(k) = \sum_{m=-\infty}^{\infty} c_{j+1}(m)g(m-2k)$$

Equations (14) and (15) show that the coefficients at a coarser level can be obtained by passing the finer level coefficients through the filter bank followed by a down-sampling of two.

By using c_j and d_j coefficients it is possible to synthesise the signal:

$$y(t)=\sum_{k=-\infty}^{\infty} c_j(k)2^{\frac{j}{2}}\varphi\left(2^j t-k\right)+ \sum_{k=-\infty}^{\infty} d_j(k)2^{\frac{j}{2}}\psi\left(2^j t-k\right) \qquad (16)$$

This separates the signal in two components, one which gives information about the details and the other one which gives information about the allure of the signal. The decomposition can be repeated several times in order to determine the allure and details for different resolutions.

3.2. APF reference generation using multiresolution analysis

A three phase currents system is transformed in a two phase system by the Clarke transform (equation 1). In the case of a distorted line current, i_α and i_β will contain the harmonic components as well (figure 5).

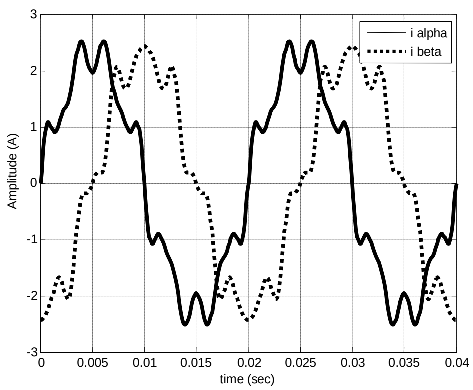

Fig.5. Harmonic distortions of i_α and i_β

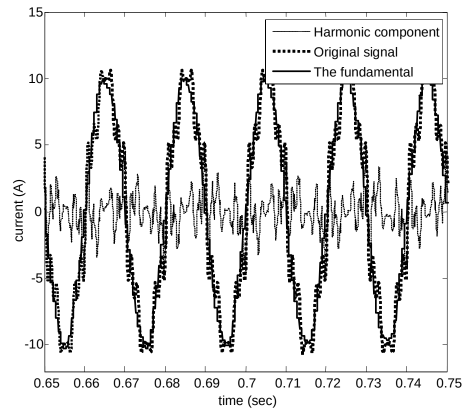

Fig.6. Signal decomposition in allure and detail

In order to generate the reference signal for the control block these currents are decomposed using multiresolution analysis and the component corresponding to the details are used to synthesise only the details of the signal up to an arbitrary set level (figure 6).

4. SIMULATION RESULTS

A Matlab/Simulink model was created for testing the proposed control structure. The model is presented in figure 7.

A rectifier was considered as nonlinear load. The DC-link voltage is calculated from the three-phase filter currents and the state of the switches, using a block that models the equation:

$$u_{DC}=\frac{1}{C}\int i(t)\,\mathrm{d}t \qquad (17)$$

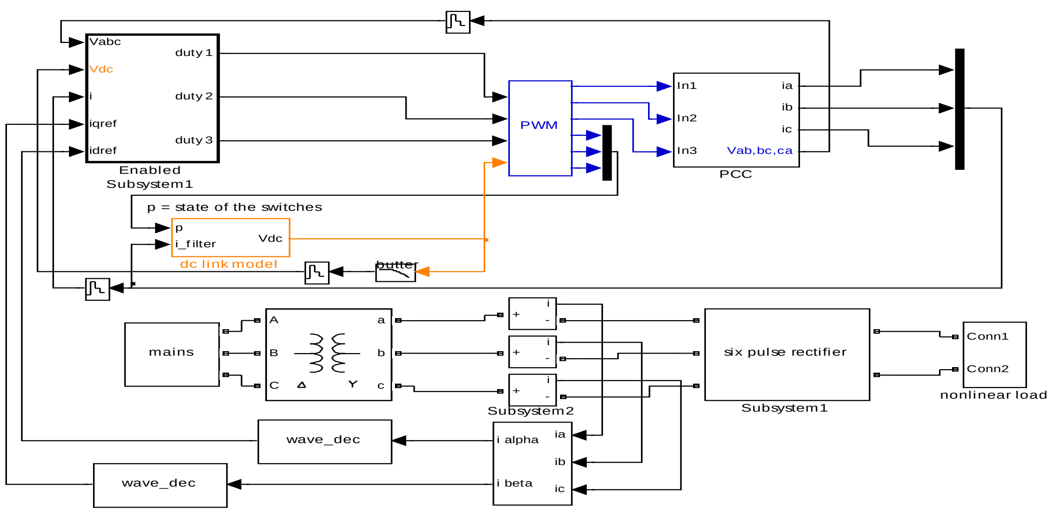

Fig.7. Simulation model

The PWM block is built using the IGBT model from SymPower System Blockset and it takes into account the blanking time.

The PCC (Point of Common Coupling) block models the mains and the filter inductors using transfer functions. Voltage harmonics similar to those measured at the mains were also taken into account to increase the accuracy of the model.

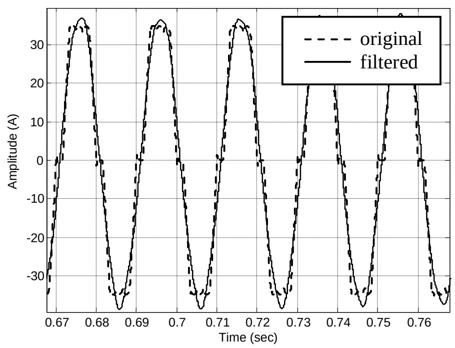

Fig.8. Stationary frame current, α axis

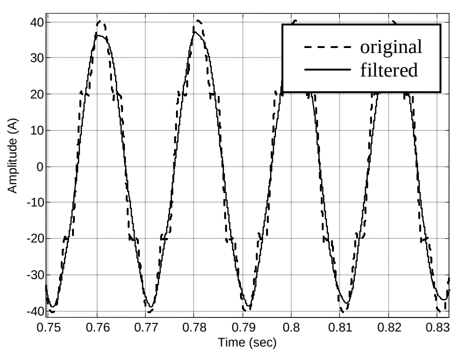

Fig.9. Stationary frame current, β axis

By using the multiresolution analysis it is possible to separate the fundamental component of the current and subsequently to obtain the reference for the APF.

The APF line current obtained is presented in figure 10. The mains current which satisfies the relation:

$$(18)\quad i_m(t) = i_F(t) + i_L(t)$$

is presented in figure 11.

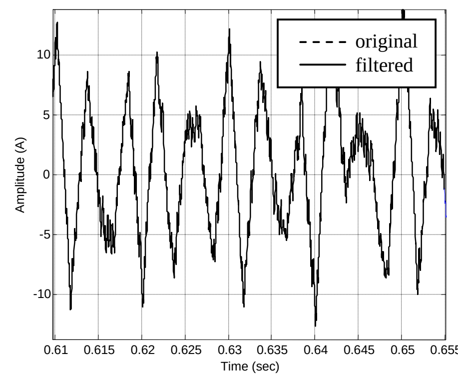

Fig.10. APF line current

There is a step change in the nonlinear load's current amplitude.

The total harmonic distortion is 28% for the nonlinear load's current and 5% after the de-noising using the APF. The THD is comparable with the THD obtained using classical methods, but the proposed method has an important advantage when used in weak networks or insular power systems. In this case the frequency can vary within a wide interval (usually several hertz) and in this case the wavelet analysis can lead to better results (Culea *et al.*, 2000).

To underline the difference between the two methods, a 49 Hz sinusoid is analysed using FFT and multiresolution analysis.

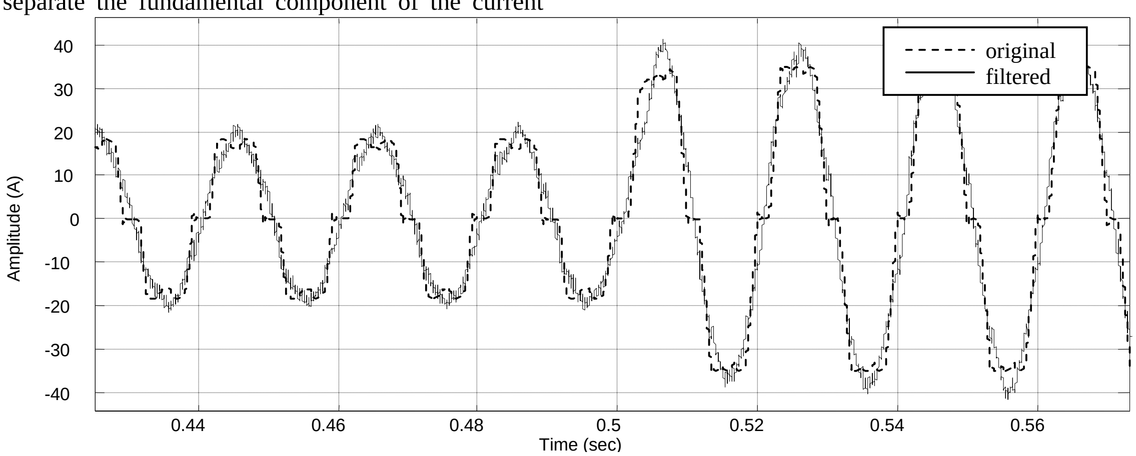

Fig.11. Nonlinear load line current and mains current after filtering

The FFT is calculated using a number of points corresponding to a 40 msec time window, suitable for analysing a 50 Hz frequency signal. Since the frequency is different, there aren't an integer number of periods within the time window and this determines the apparition of higher order harmonics in the amplitude spectrum. Recomposing the signal using this amplitude spectrum with IFFT leads to the result presented in figure 12.

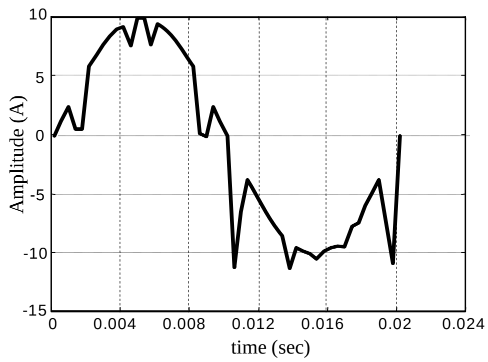

Fig.12. FFT errors induced by the frequency deviation

The same 49 Hz sinusoid analysed using wavelets decomposition is recomposed using the inverse transform without major alteration, as it can be seen in figure 13.

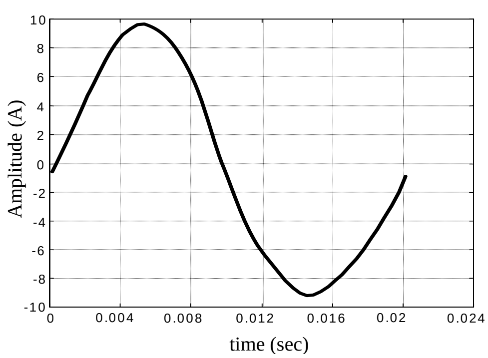

Fig.13. Signal re-composition using multiresolution analysis

5. CONCLUSIONS

The paper presents a control structure for APF. Signal decomposition by multiresolution analysis was used in order to improve the performances of the APF when the mains' frequency is varying around 50 Hz.

The method leads to satisfactory results, similar to those obtained using classical methods (like Fourier analysis) which are however sensitive to variations in fundamental frequency.

Future work should consider the effect of the delays introduced by the algorithm on the performances of the APF and whether or not a power factor correction method can also be implemented.

6. REFERENCES

H Akagi (1995), New trends in active filters, *European Power Electronics Conf. Proc.*, pp17-21

S.C. Burrus, R.A. Gopinath, and H.Guo (1997), *Introduction to Wavelets and Wavelet Transform*, Prentice Hall, New Jersey

Burrus, C. S. and R. A. Gopinath, H. Guo. Introduction To Wavelets And Wavelet Transforms, A Primer. Upper Saddle River, NJ Prentice Hall, 1998

S. Buso, L. Malesani, P. Mattavelli, (1998) Comparison of Current Control Techniques for Active Filter Applications , *IEEE Trans. on Ind. Electronics*, **vol. 45**, No. 5, pp. 722-729.

D Butt, M Sumner and J C Clare (1999), Harmonic compensation in active shunt filters using controllers employing rotating frames of reference, Proc EPE'99 Lausanne, CD-ROM

M. Culea, D. Aiordachioaie, M. Gaiceanu (2000) On the Harmonic Reduction Using Wavelet Based Signal Processing, *The Annals of "Dunarea de Jos" University of Galati*, **Fascicle III**, pp 12-16

RC Dugan, MF McGranaghan, and HW Beaty (1996), *Electrical power systems quality*, McGraw-Hill

H. Fujita and H. Akagi (1991), A Practical Approach to Harmonic Compensation in Power Systems Series connection of Passive and Active Filters, *IEEE Transactions on Industry Applications*, **Vol: 27** Issue: 6, Page(s): 1020 –1025.

Z Lu and TC Green (1998), Neural network based predictive control strategy of a shunt active power filter for electric drives, *IEE Power Electronics and Variable Speed Drives Conference*, pp287-291

L Malesani, P Mattavelli and P Tomasin (1997), High performance hysteresis modulation technique for active filters, *IEEE Transactions on Power Electronics*, **Vol.12**, No. 5, pp876-884

M. Rastogi, R. Naik and N. Mohan (1994), A Comparative Evaluation of Harmonic Reduction Techniques in Three-Phase Utility Interface of Power Electronic Loads, *IEEE Transactions on Industry Applications*, , **Vol: 30** Issue: 5, Page(s): 1149 –1155.

Y. Sato, T. Kawase, M. Akiyama, and T. Kataoka (1999), A control strategy for general purpose active filters based on voltage detection, *IEEE Industrial Applications Society Annual Meeting*, **vol. 1**, Phoenix, Arizona, USA, pp. 471-478

D. N. Zmood, D. G. Holmes (2003), Stationary Frame Current Regulation of PWM Inverters with Zero Steady-State Error *IEEE Trans. on Power Electronics*, **vol. 18**, no. 3, pp. 814 – 822